Visible-light photocatalysis in nitrogen–carbon-doped TiO_2 films obtained by heating TiO_2 gel–film in an ionized N_2 gas

Jing Yang, Haizan Bai, Qing Jiang, Jianshe Lian *

Key Lab of Automobile Materials, Ministry of Education, College of Materials Science and Engineering, Jilin University, Changchun, 130025, China

Abstract

To use solar irradiation or interior lighting efficiently, we sought a photocatalyst with high reactivity under visible light. Nitrogen and carbon doping TiO_2 films were obtained by heating a TiO_2 gel in an ionized N_2 gas. The as-synthesized $TiO_{2-x-y}N_xC_y$ films have shown an improvement over titanium dioxide in optical absorption and photocatalytic activity such as photodegradation of methyl orange under visible light. The process of the oxygen atom substituted by nitrogen and carbon was discussed. Oxygen vacancy induced by the formation of Ti^{3+} species and nitrogen and carbon doped into substitution sites of TiO_2 have been proven to be indispensable for the enhance of photocatalytic activity, as assessed by UV–Vis Spectroscopy and X-ray photoemission spectroscopy.
© 2007 Elsevier B.V. All rights reserved.

1. Introduction

Photoinduced oxidation and reduction reactions at the surface of TiO_2 particles or thin films have been attracting much attention in view of their possible applications for photo electrochemical splitting of water into hydrogen and oxygen [1,2], wet solar cells [3] and photocatalysis [4–6]. Its unique photocatalytic properties make it suitable for the oxidation of organic pollutants and other contaminants from wastewater or drinking water supplies [7–10]. When TiO_2 is illuminated with light at wavelength <390 nm, the generation of electron/hole pairs makes it possible to be applied as a photocatalyst. The valence band potential is positive enough to generate hydroxyl radicals at the surface, and the conduction band potential is negative enough to reduce molecular O_2. The hydroxyl radical is a powerful oxidizing agent and attacks organic pollutants presenting at or near the surface of the TiO_2 resulting in complete oxidation to CO_2.

However, one disadvantage of TiO_2 is that it can only absorb UV light. It is generally recognized that the improved photocatalysts should allow the use of the main part of solar spectrum and even poor illumination of interior lighting. Therefore, the major aim in the development of TiO_2-based materials is to extend the photoactivity from 3.2 eV into visible light range in order to utilize solar light more efficiently. One approach was to dope transition metals into TiO_2 [11–13], and another was to form reduced TiO_x photocatalysts [14,15]. Recently, doping of polycrystalline powders and films of TiO_2 with anion impurities such as nitrogen [16–18] carbon [19] and sulfur [20] has been shown to be effective in lowering the threshold energy for photochemistry on the TiO_2 surface. For example, Asahi et al. [17,18] have accomplished N-doping by reactive sputtering of TiO_2 film targets in N_2/Ar gas mixtures, by high-temperature treatment of TiO_2 powders in NH_3/Ar atmospheres, and by oxidative annealing of TiN powder. In these cases, a noticeable absorption range for light at energy less than the band-gap energy of 3.0 eV has been observed and the films and powders of $TiO_{2-x}N_x$ showed a dramatic improvement over pure titanium oxide under visible light in their optical absorption and the level of photocatalytic activity. Khan et al. [19] synthesized a chemically modified n-$TiO_{2-x}C_x$ by controlled combustion of Ti metal in a natural gas flame. This material, in which carbon substituted for some of the lattice oxygen atoms, absorbed light at

---

* Corresponding author. Tel.: +86 431 85095875; fax: +86 431 85095876.
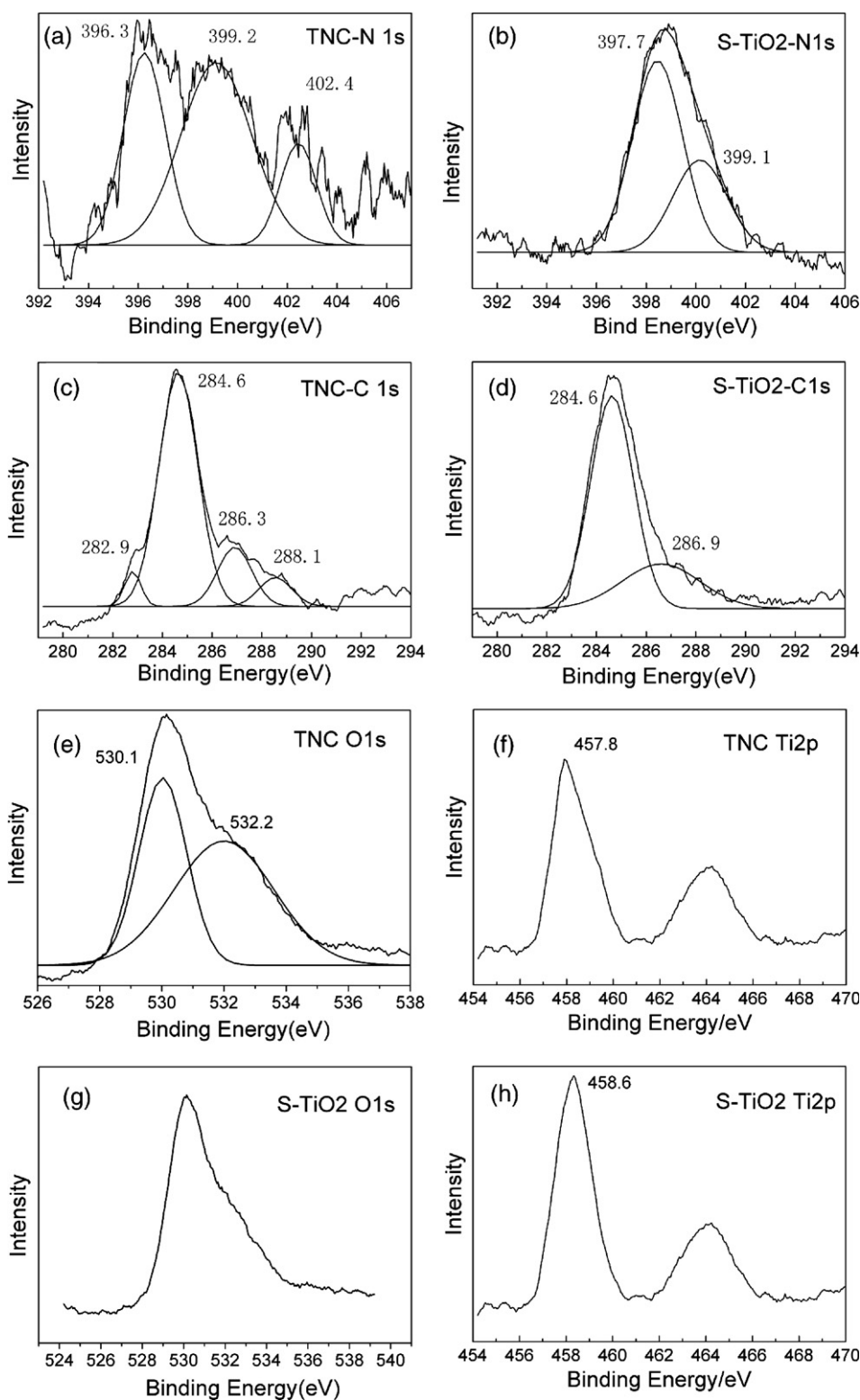*E-mail address:* lianjs@jlu.edu.cn (J. Lian).

Fig. 1. The N (1s), C (1s), O (1s) and Ti (2p) core levels of TNC film and *s*-TiO2 film. (a) The N (1s) core levels with three peak structures at binding energies of 402.4 eV, 399.2 eV, and 396.3 eV of TNC film; (b) The N (1s) core levels with two peak structures at binding energies of 397.7 eV and 399.1 eV of *s*-TiO$_2$ film; (c) The C (1s) core levels with four peak structures at binding energies at 288.1 eV, 286.3 eV, 284.6 eV and 282.9 eV of TNC film; (d) The C (1s) core levels with two peak structures at binding energies at 288.1 eV and 286.3 eV of *s*-TiO$_2$ film; (e) The O (1s) core levels at binding energies at 530.1 eV and 532.2 eV of TNC film; (f) The Ti (2p) core levels at binding energy at 457.8 eV of TNC film.

wavelengths below 535 nm and had evident lower band-gap energy than tutile (2.32 eV versus 3.00 eV).

In our study, nitrogen and carbon doping in TiO_2 film were obtained by a method of heating the TiO_2 gel in an ionized N_2 gas. Through the substitution of some of the lattice oxygen atoms by nitrogen and carbon in the TiO_2 film simultaneously, an enhanced absorption of visible light would be expected. The formation mechanism of the oxygen atom substituted by nitrogen and carbon atoms in the film and the influence of nitrogen and carbon in the doped TiO_2 film on the absorption and photocatalytic activity were investigated.

2. Experimental details

Titanium isopropoxide $Ti(OC_4H_9)_4$ (97%), ethanol (99.7%), acetic acid and 2,4-Pentanedione (acetylacetone) were used as precursor in the formation of TiO_2 sol. The as-called solution A was made by adding 8.5 ml titanium isopropoxide and 0.5 ml 2,4-pentanedione into 29.5 ml ethanol. Solution B was prepared by mixing 29.5 ml of ethanol, 2 ml acetic acid and 2 ml de-ionized water together. Solution B was then added gradually into solution A by stirring at 318 K. Then the mixed solution was further stirred for 40 min at 318 K. The acetylacetone (AcAc) was used to chelate titanium alkoxide, to form a monomeric complex [21]. The chelation of AcAc is to inhibit the hydrolysis of titanium alkoxide.

The precursor TiO_2 films were prepared on glass substrates. The glass substrates were carefully cleaned first with ethanol and then with acetone in an ultrasound bath. A dip-coating apparatus was used to coat the TiO_2 sol on the glass substrates. The dip-coating apparatus can take the substrate to dip into the sol and then rise up slowly. The sol can be coated on the substrate homogeneously.

Then the gel films of TiO_2 were obtained by drying the sol at 80 °C for 10 min. The coating process was repeated five times to insure that the thickness of the thin film is suitable for various analyses. The doping of nitrogen and carbon into the lattice of TiO_2 crystals was achieved in a chamber inflated with in an ionized N_2. The gel films of TiO_2 were put in the chamber that was then vacuumized. The N ions were obtained by using ionization equipment and then inputted into the vacuum chamber with the pressure of 1.0 Pa. The gel films of TiO_2 were heated at 500 °C for 2 h to obtain the $TiO_{2-x-y}N_xC_y$ film (abbreviation: TNC film in the following). For comparison TiO_2 gel film was calcined at 500 °C for 2 h in air to obtain the normal TiO_2 film (s-TiO_2).

The phase structures of the as-synthesized films were analyzed by X-ray diffraction (XRD) (D/MAX 2500PC) with CuKα radiation in the range 10–60° (2θ). The thickness of the film was about 1 μm measured using Tangent Profilometer (Dektak 16000, Veeco, USA). In order to investigate the nitrogen and carbon states in TNC film, the XPS spectra of the films were acquired with an ESCALAB Mk II (Vacuum Generators) spectrometer using unmonochromatized AlKα X-rays (240 W). Cycles of XPS measurements were done in a high-vacuum chamber with a base pressure of 10^{-8} Torr. The UV–Visible Spectroscopy (Spectroscopy 752PC) was used to

measure the absorbance of the as-synthesized films and to confirm the band gap of different TiO_2 films.

The photocatalytic activity experiments on both the TNC and TiO_2 films for the methyl orange in air were performed at ambient temperature. The visual light source was a 500 W Hg lamp (100 mm long) used for daily lighting, which was surrounded by a circulating water jacket to cool the lamp. Typically, the films were put into the aqueous solution containing methyl orange 20 mg/l. All runs were conducted at ambient pressure and temperature. The distance between the Hg lamp and the reactor was 30 cm for each experiment. The reaction mixture was exposed to the Hg lamp. After irradiation the methyl orange was analyzed using UV–Visible (UV–vis) Spectroscopy. The decolorization of methyl orange, at its absorption maximum (445 nm), was recorded as a function of time.

3. Results and discussion

3.1. The structural analysis and N, C, O and Ti states in the TNC films

The presence of nitrogen and carbon ions on the surface of TNC film was revealed by XPS (Fig. 1). The N (1s) core levels (Fig. 1a) of TNC film revealed three peak structures at binding energies of 402.4 eV, 399.2 eV, and 396.3 eV, respectively. Saha and Tompkins [22] investigated the N (1s) XPS spectrum during the oxidation process of TiN and assigned their three peaks of XPS spectrum as the atomic β-N (396 eV) and the molecularly chemisorbed γ-N_2 (400 eV and 402 eV), respectively. In the spectrum of TNC film the peak at the higher binding energy of 402.4 eV was attributed to molecularly adsorbed nitrogen species, the peak at lower binding energy of 399.1 eV was attributed to C–N bonds, and the nitrogen peak at 396.3 eV was assigned to the N–Ti bonds. In consideration of the nitrogen component related to the 396.3 eV peak, the XPS spectrum proved that nitrogen was doped in the near-surface region of TNC film. The XPS spectrum for the s-TiO_2 film was also shown in Fig. 1b. The s-TiO_2 film also included small amount of N. However, only two peaks of 397.7 eV and 399.1 eV were found and the peak at 396.3 eV of N (1s) was not observed, which indicated that the presence of N was due to the surface absorption of N_2 in air during the preparation of samples for XPS measurements and there was no N doped into the s-TiO_2 films.

The C (1s) core levels of TNC film revealed four peak structures at binding energies of 288.1 eV, 286.3 eV, 284.6 eV and 282.9 eV, respectively, shown in Fig. 1c. Hashimoto and co-workers [23] prepared carbon-doped titania by oxidizing TiC, and observed C (1s) XPS peak with much lower binding energy (281.8 eV). They assigned this C (1s) XPS peak to be Ti–C bond in carbon-doped anatase titania by substituting some of the lattice oxygen atom with carbon. In our experiment, the two features of 288.1 eV and 286.3 eV at the higher binding energies were attributed to C–N bond and C–O bond, respectively, and the carbon peak at 284.6 eV was assigned to the C remained in the precursor organic compound and the carbon peak at 282.9 eV

was attributed to the C–Ti binding which represented that carbon was doped into substitutional sites of O in TiO_2. We also observed the C (1s) of the XPS spectrum for the s-TiO_2 films (Fig. 1d). The peak at 284.6 eV was assigned to the C remained in the precursor organic compound and that at 286.9 eV to the C–O bond. However, the peak at 282.9 eV of C (1s) was not observed which indicated that there was no C–Ti bond formed in the s-TiO_2 film. Therefore, the above XPS spectra proved that both nitrogen and carbon were doped into the near-surface region of TNC film and replaced O to form N–Ti bonds and C–Ti bonds, respectively.

The O (1s) XPS spectra in Fig. 1e and g also show significant changes upon nitrogen and carbon incorporation. The O (1s) peak in the TNC films appears at 530.1 eV and 532.4 eV. The peak at 532 eV is a feature that was first observed by Saha and Tompkins [22] and was most recently characterized by Gyorgy et al. [24] in their depth profiling study on TiN surfaces. Gyorgy et al. assigned this feature to the formation of oxidized Ti–N, which leads to the Ti–O–N structure. Because of the surface strain and lattice distortion which may form in the synthesized TNC film, the surface of the film was relaxed and any doping poses a steric problem [25] which is also suggested by the significant shifts in the XPS binding energies. Therefore it is not surprising that one observes a much higher binding energy of the Ti 2p and O (1s) in some doped film [25–26]. The structure of the TNC film in our experiment is such that the doping of nitrogen and carbon disturbs the TiO_2 lattice and changes the Ti–O bond, shifting the infrared transitions to higher energy. The doping of carbon may contribute to higher energy than the peak of 532 eV for the nitrogen doped TiO_2 observed by Saha and Tompkins [22], because the C and N doped structures are considerably strained [27]. The nitrogen and carbon, which is incorporated to form the O–Ti–N and O–Ti–C structure, should shift the O–Ti–O infrared feature to higher frequencies. Therefore, the appearance of the peak at 532.4 eV is a consistent feature for the nitrogen and carbon substitution in TiO_2 and signifies the formation of an O–Ti–N–C structure.

The XPS spectrum of Ti 2p in the TNC film can be fitted as one peak at 457.8 eV (Fig. 1f). Compared to the binding energy of Ti^{4+} in pure anatase titania (458.6 eV, Fig. 1h), there is a slight red-shift of 0.8 eV for the TNC film, which suggests that Ti^{3+} species was formed in the nitrogen and carbon-doped titania [28].

XPS spectra proved that both nitrogen and carbon were doped into the near-surface region of TNC film and replaced O to form N–Ti and C–Ti bindings, respectively. The nitrogen and carbon concentration were estimated from the relative area intensities of the N (1s), C (1s), Ti (2p), and O (1s) peaks. They were normalized with respect to the relative sensitivity factors in the Vacuum Generators software package. XPS data indicated an average composition of the TNC film to be $TiO_{2-x-y}N_xC_y$, where x is 0.14 and y is 0.48 according to the areas of the Ti–N, Ti–C and Ti–O peaks. Therefore, the stoichiometric composition of the as deposited TNC film is $TiO_{1.38}N_{0.14}C_{0.48}$. Thus, the observed changes in the XPS spectra are providing consistent structural information for O–Ti–N and O–Ti–C formation, i.e., the substitution doping of nitrogen and carbon for oxygen, which leads to the enhanced photocatalytic activity in TNC film.
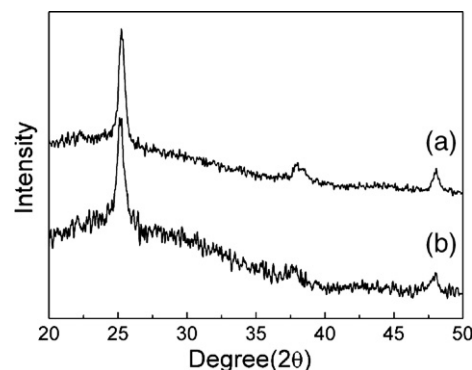

Fig. 2. The X-ray diffraction (XRD) pattern of s-TiO_2 film (a) and TNC film (b).

Fig. 2 shows the XRD patterns of TNC film and s-TiO_2 film. The upside spectrum is the XRD pattern of s-TiO_2 film, where the diffraction peaks of (101), (004) and (200) planes of the tetragonal anatase structure of TiO_2 were observed. And the underside spectrum is that of TNC film which has almost the same spectrum with that of the s-TiO_2 film. The amorphous peaks were the peaks of the glass substrate. Because of the small thickness, the weak peaks of the film are not clearly distinguished. The results clearly indicate that both films are crystallized to the tetragonal anatase phase. The very small differences in lattice spacing between TiO_2 and $TiO_{2-x-y}N_xC_y$ are not distinguished by the XRD analysis due to the slight quantities of doping.

Reduced metal oxides can be formed through the thermal creation of O vacancies and metal interstitials in originally stoichiometric metal oxides [29]. These defects act as donors of electrons and have a profound influence on the chemical and electrical behavior of transition metal oxides. Here, we focus on the reaction process to form the reduced TiO_2 substituted by nitrogen and carbon atoms during the process of heating TiO_2 gel in the ionized N_2.

The hydrolysis of titanium alkoxide Ti $(OC_4H_9)_4$ followed by condensation is involved in this sol–gel process [30]:

$$Ti(OR)_4 + 4H_2O \rightarrow Ti(OH)_4 + 4ROH \tag{1}$$
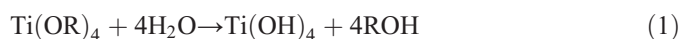
where: $R=C_4H_9$, then after heating at 500 °C:

$$Ti(OH)_4 \rightarrow TiO_2 + 2H_2O \tag{2}$$

The thermal decomposed products of organic compound should be CO_2, H_2O and the residual carbon existed in the precursor organic compound of TiO_2 gel, which facilitated the incorporation of carbon in the n-TiO_2 films. The residual carbon and hydrogen may participate to the reduction of TiO_2. The XPS spectrum of Ti 2p in the TNC film suggests that Ti^{3+} species was formed in the nitrogen and carbon-doped titania, i.e.:

$$2TiO_2 + C \rightarrow Ti_2O_3 + CO \tag{3}$$

Reaction (3), however, is not a direct one. It proceeds through several successive steps that overlap at high temperature [31]

$$TiO_2 - Ti_5O_9 - Ti_4O_7 - Ti_3O_5 - Ti_2O_3 \tag{4}$$

At the same time CO was also ionized by the ionization equipment to form C ions. Further, the oxygen sites were
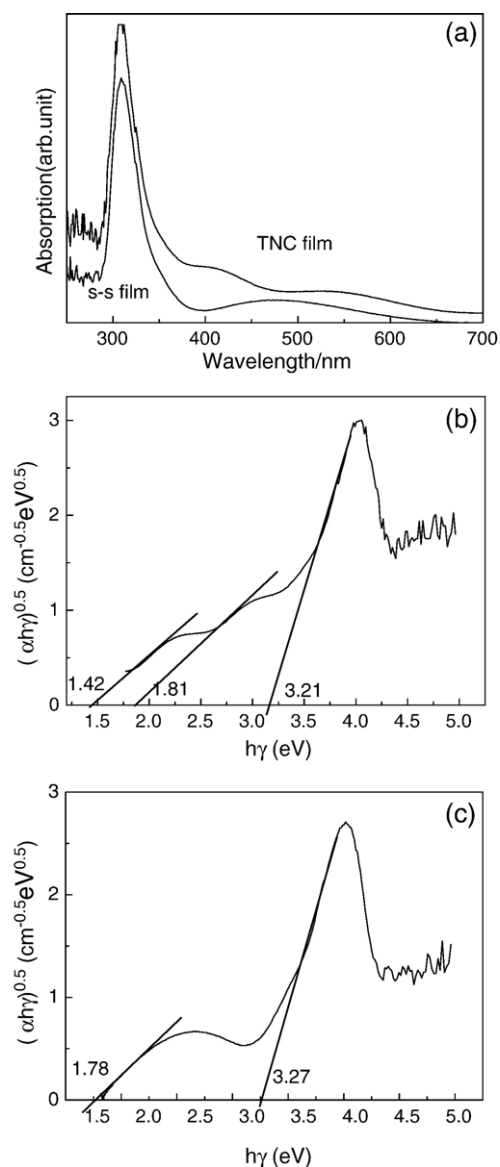
Fig. 3. The UV–visible spectra (a) of TNC film and the reference *s*-TiO$_2$ film and variation of $(\alpha h\gamma)^{0.5}$ with excitation energy (hν) for the TNC film (b) and *s*-TiO$_2$ film (c) to identify indirect transitions. The TNC film (b) shows three threshold wavelengths of at 355 nm (ultraviolet range), 541 nm and 705 nm, (visible range) with higher absorption which corresponds to a band-gap energy of 3.21 eV, 1.81 eV and 1.42 eV. The *s*-TiO$_2$ film (c) shows only two threshold wavelengths at 351 nm and 642 nm, which corresponds to the band-gap energy of 3.27 eV and 1.78 eV, respectively. And the absorption of *s*-TiO$_2$ film was lower than that of TNC film.

substituted by N and C to form a complex (Ti$_2$O$_3$–TiN–TiC) solid solution which has the same crystalline structure as TiO$_2$. Hence we can infer that TNC film is an interstitial phase, with oxygen atoms being substituted by nitrogen and carbon atoms in its lattice sites. When TiO$_2$ is reduced by heating in the ionized N and C, O vacancies are formed, which take the form of missing O atoms in the bridging O rows at the surface. The surface O vacancies constitute the most abundant surface donor [32–34] below the conduction band and act as adsorption sites for simple molecules such as CO and O$_2$ [35]. Ti interstitials, which are also formed, are mainly present in the film where they

control the film electronic properties of the reduced material at low temperatures [36].

Asahi et al. [17] have associated the high catalytic activity that they observed with the bonding of atomic nitrogen to titanium determined by the N (1s) XPS peak at 396 eV. While in our experiment, XPS peaks of N (1s) at 396 eV and C (1s) at 282.9 eV were observed in the TNC film, which indicates that our method was more efficient and easy for the doping of both N and C into TiO$_2$ films. Because of ionic charge compensation [37], the N and C acceptors can easily be compensated by donor levels, which are related to additional oxygen vacancies and cautions. Thus, we speculate that the doping of N and C ions into the TiO$_2$ lattice and substituting O atoms should increase the local concentration of electronically reduced Ti^{3+} states due to the monovalent oxidation state of the nitrogen anion.

3.2. The UV–visible absorption and band gap of both films

The UV–visible absorption measurements, as shown in Fig. 3a, indicate that the TNC film noticeably absorb the light in the visible range and has high absorbance, whereas the absorbance of *s*-TiO$_2$ film was much lower than that of the TNC film.

Assuming that the fundamental absorption of the TiO$_2$ crystal possesses an indirect transition [29], these spectra were analyzed to obtain the band-gap energy, E_g, from the expression corresponding to indirect gap semiconductors,

$$\alpha(h\nu)h\nu \propto (h\nu - E_g)^2. \tag{5}$$

Here α is the absorption coefficient (cm^{-1}) and hν (eV) is the energy of excitation. From the plots shown in Fig. 3b and c, the intercepts defining the energy gaps E_g of different films are obtained. The TNC film shows three optical absorption thresholds at 355 nm (ultraviolet range), 541 nm and 705 nm, (visible range) with the higher absorbance which corresponds to band-gap energy of 3.21 eV, 1.81 eV, 1.42 eV, respectively (Fig. 3b), whereas the reference *s*-TiO$_2$ shows only two at 351 nm and 642 nm, which corresponds to band-gap energy of 3.27 eV and 1.78 eV, respectively (Fig. 3c). The broad absorption band around 480 nm is probably the absorption of the remained C in the film, so it does not mean that *s*-TiO$_2$ also can absorb the visual light.

Three absorption thresholds of TNC film indicate three possible compositions of chemically modified TiO$_2$, which is due to the doping of the nitrogen and carbon. As we found N and C doping in the TiO$_2$ film from the analysis of XPS, therefore, we deduced that the band-gap energy of 1.81 eV is attributed to the N-doping and the band-gap energy of 1.42 eV is assigned to the C-doping. While the band-gap energies of other

Table 1
The band-gap energies comparison at the range of visual light of different doping TiO$_2$

Doping atom	Nitrogen [a]	Carbon [b]	Nitrogen and carbon [c]
Band-gap energy (eV)	1.14	2.32	1.81 and 1.42

[a] Reference [17].
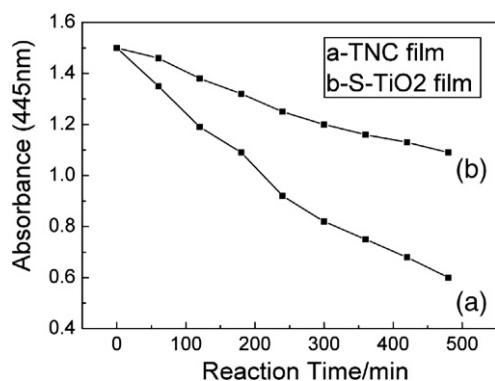[b] Reference [19].
[c] In our experiment.

Fig. 4. The photodegradation effect of TNC film and s-TiO$_2$ film by measuring the absorbance decrease of the methyl orange with the increase of the time at its absorption maximum (445 nm) using UV–Visible (UV–vis) Spectroscopy.

research about N-doping and C-doping had only single optical absorption threshold at visual light range (Table 1). In our experiment, two optical absorption thresholds will certainly enhance the absorption of the visual light and hence increase the photocatalytic activity.

The shift of the photodesorption threshold energy to the blue could easily be explained by the doping of the nitrogen and carbon [36]. A well-known phenomenon associated with the optical properties of n-type semiconductor is the so-called "band-filling mechanism" [35]. It is based on the effect of electron concentration on the location of the Fermi level, E_f. For intrinsic or lightly doped semiconductors, such as vacuum-annealed and thermally reduced TiO$_2$, E_f is positioned within the band gap and the semiconductor is said to be nondegenerate. When the electron concentration in the bulk is increased, e.g., by heavy n-type doping, E_f lies above the bottom of the conduction band and the semiconductor becomes degenerate. As a consequence, some of the states within the conduction band (CB) are then filled, and electrons excited by a UV–visible photon must go into higher levels in order to enter the CB, thus leading to a blueshift in optical absorption. In our experiment, two optical absorption thresholds were measured in the TNC film, which is due to the doping of nitrogen and carbon in the TiO$_2$. Therefore, the blueshift of the photodesorption threshold energy is attributed to the band-filling mechanism based on the increase of the n-doping level of the TiO$_2$ crystal by N and C incorporations.

3.3. Photocatalytic activity and the photocatalytic mechanisms

The wavelength of maximum absorption of methyl orange to visual light is at about 445 nm. So we measured the variation of absorbance of methyl orange solution with time at 445 nm. The mechanism of the photo degradation of methyl orange is that the methyl orange was degraded into CO$_2$ and H$_2$O by the TNC film (or TiO$_2$ film) under the irradiation of visual light. The absorbance and its decrease of the methyl orange solution were then used to evaluate the photodegradation of the tested films. Fig. 4 demonstrates the photodegradation observed for methyl orange in the presence of the doped TNC film and undoped s-TiO$_2$ film to measure the degradation effect in normal

environments. The data for the TNC film showed a notably enhanced photocatalytic activity for methyl orange. In contrast, the undoped s-TiO$_2$ film showed moderate activity under visible light radiation. Therefore, the photodegradation effect of TNC film was much better than that of s-TiO$_2$ film.

It was reported [17] that reduced TiO$_2$ introduces localized oxygen vacancies whose valence states located at about 0.75–1.18 eV below the conduction band edge of TiO$_2$, which result in higher sensitivity of the reduced TiO$_x$ photocatalyst to visible light. Based on our of UV–vis and XPS results, it is concluded that the presence of Ti^{3+} species produced in the process of gel transition and heating in the ionized N$_2$ leads to the formation of oxygen vacancy in the as-synthesized TNC film, which results in the sensitivity to visible light and high photocatalytic activity under visible light of the as-synthesized doped titania. Therefore, the visible light photocatalytic activity can also be ascribed to the presence of oxygen vacancy states because of the formation of Ti^{3+} species between the valence and the conduction bands in the TiO$_2$ band structure.

Our UV–vis experiments showed that the nitrogen–carbon-doped titania has an obvious absorption up to 700 nm and has two optical absorption thresholds at 1.42 eV and 1.81 eV, which also can increase the photocatalytic activity under visible light of TNC film. Therefore, we conclude that the two mechanisms, existence of the oxygen vacancy induced by Ti^{3+} and nitrogen and carbon doping, are both responsible for the visual light response and the better photocatalytic activity occurring in our experiments.

4. Conclusion

Nitrogen–carbon-doped TiO$_2$ films were obtained by heating a TiO$_2$ gel in an ionized N$_2$ gas. TNC films have shown an improvement in optical absorption and photocatalytic activity such as photodegradations of methyl orange over s-TiO$_2$ under visible light. The visible light photocatalytic activity is ascribed to the presence of oxygen vacancy states because of the formation of Ti^{3+} species in the band structure. Nitrogen and carbon doped into substitutional sites of TiO$_2$ has also proven to be indispensable for band-gap narrowing and photocatalytic activity.

Acknowledgments

References

[1] A. Fujishima, K. Honda, Nature 238 (1972) 37.
[2] S.U.M. Khan, J. Akikusa, Int. J. Hydrogen Energy 27 (2002) 863.
[3] B. O'Regan, M. Gratzel, Nature 353 (1991) 737.
[4] A. Linsebigler, G. Lu, J.T. Yates Jr., Chem. Rev. 95 (1995) 735.
[5] S.T. Martin, W. Choi, D.W. Bahnemann, M.R. Hoffmann, Chem. Rev. 95 (1995) 69.
[6] N. Serpone, E. Pilezzetti, Photocatalysis: Fundamentals and Applications, Wiley-Interscience, New York, 1989.
[7] G.P. Fotou, S.E. Pratsinis, J. Aerosol Sci. 26 (1995) 227.

[8] K.Y. Jung, S.B. Park, Appl. Catal., A 224 (2002) 229.
[9] B. Bems, F.C. Jentoft, R. Schlogl, Appl. Catal., B 20 (1999) 155.
[10] J.M. Hermann, C. Guillard, J. Disdier, C. Lehaut, J. Appl. Catal., B 49 (2002) 189.
[11] A.K. Ghosh, H.P. Maruska, J. Electrochem. Soc. 124 (1977) 1516.
[12] W. Choi, J. Phys. Chem. 98 (1994) 13669.
[13] M. Anpo, Catal. Surv. Jpn. 1 (1997) 169.
[14] R.G. Breckenridge, W.R. Hosler, Phys. Rev. 91 (1953) 793.
[15] D.C. Cronemeyer, Phys. Rev. 113 (1959) 1222.
[16] S. Sato, Chem. Phys. Lett. 123 (1986) 126.
[17] R. Asahi, T. Morikawa, T. Ohwaki, K. Aoki, Y. Taga, Science 293 (2001) 269.
[18] T. Morikawa, R. Asahi, T. Ohwaki, K. Aoki, Jpn. J. Appl. Phys. 40 (2001) 561.
[19] S.U.M. Khan, M. Al-Shahry, W.B. Ingler Jr., Science 297 (2002) 2243.
[20] T. Umebayashi, T. Yamaki, H. Itoh, K. Asai, Appl. Phys. Lett. 81 (2002) 454.
[21] J. Livage, C. Sanchez, J. Non-Cryst. Solids 145 (1992) 11.
[22] N.C. Saha, H.G. Tompkins, J. Appl. Phys. 72 (1992) 3072.
[23] M. Miyauchi, A. Ikezawa, K. Hashimoto, Phys. Chem. Chem. Phys. 6 (2004) 865.
[24] E. Gyorgy, A. Perez del Pino, P. Serra, Surf. Coat. Technol. 173 (2003) 265.
[25] J.A. Rodriguez, T. Jirsak, J. Dvorak, S. Sambasivan, D. Fischer, J. Phys. Chem., B 104 (2000) 319.
[26] H. Irie, Y. Watanabe, K. Hashimoto, Chem. Lett. 32 (2003) 772.
[27] X. Zhang, M.X. Wang, L. Qu, X. Peng, Appl. Phys. Lett. 81 (2002) 2076.
[28] X. Chen, C. Burda, J. Phys. Chem., B 108 (2004) 15446.
[29] S. Lee, C. Jeon, Chem. Mater. 16 (2004) 4892.
[30] T. Yoko, L. Hu, H. Kozuka, S. Sakka, Thin Solid Film 283 (1996) 188.
[31] G. Zhang, O. Ostrovski, Mater. Sci. Eng., B 31 (2000) 129.
[32] R.L. Kurtz, R. Stockbauer, T.E. Madey, Surf. Sci. 218 (1989) 178.
[33] M.A. Henderson, Surf. Sci. 400 (1998) 203.
[34] U. Diebold, Surf. Sci. Rep. 48 (2003) 53.
[35] E. Yagi, R.R. Hasiguti, M. Aono, Phys. Rev., B Condens. Matter 54 (1996) 7945.
[36] J.L. Gole, J.D. Stout, J. Phys. Chem., B 108 (2004) 1230.
[37] E.C. Lee, Y.S. Kim, Y.G. Jin, K.J. Chang, Phys. Rev., B Condens. Matter 64 (2001) 085120.